Oblique angle deposition of Au/Ti porous getter films

Ming Wu, Johan Moulin, Alain Bosseboeuf

Journal of Applied Physics

Oblique angle deposition of Au/Ti porous getter films

Cite as: J. Appl. Phys. **124**, 055301 (2018); https://doi.org/10.1063/1.5044570
Submitted: 14 June 2018 . Accepted: 17 July 2018 . Published Online: 01 August 2018

Ming Wu, Johan Moulin, and Alain Bosseboeuf

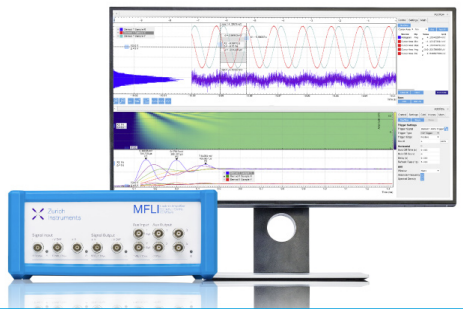

Oblique angle deposition of Au/Ti porous getter films

Ming Wu,[1,2,a)] Johan Moulin,[2] and Alain Bosseboeuf[2]
[1]*Department of Microelectronics, Soochow University, Suzhou 215006, China*
[2]*Center for Nanoscience and Nanotechnology (C2N), CNRS, Univ. Paris-Sud, Université Paris-Saclay, 91405 Orsay cedex, France*

(Received 14 June 2018; accepted 17 July 2018; published online 1 August 2018)

Interdiffusion in gold/titanium films with titanium evaporated on silicon at different oblique angles (0°, 30°, 50°, and 70°) and gold evaporated under normal incidence is investigated using a scanning electron microscope and *in-situ* sheet resistance measurements for the optimization of the films' effective gettering ability during and after a low-temperature thermal activation. Films have a tilted columnar structure and a porosity increasing with the deposition angle in agreement with calculated values. The oxygen effective gettering ability, characterized by energy-dispersive X-ray spectroscopy, increases with the deposition angle. It is shown that the gold/titanium film with titanium deposited with an oblique angle of 50° is an optimized condition to obtain the largest sorption capacity after 1 h thermal activation at temperatures lower or equal to 300 °C. This film has a low initial residual stress that becomes highly tensile if thermal activation is performed above 300 °C. *Published by AIP Publishing*. https://doi.org/10.1063/1.5044570

I. INTRODUCTION

Some applications require micro-electro-mechanical system (MEMS) devices to be packaged in a high vacuum environment. For example, high-quality factor mechanical micro-resonators or low heat loss microbolometers can only be obtained in a vacuum better than 10^{-3} mbar.[1,2] A general technological trend is to realize such a vacuum encapsulation at the wafer-level at low temperature (≤300 °C) by hermetically sealing a cap integrating a small cavity volume in the microliter range or below. To maintain a low internal pressure during the entire lifetime of the device, integration of a non-evaporable getter (NEG) in the cavity is then required.[3,4] The conventional bulk or sheet getters cannot be used for these small size packages.[5] Consequently, integrating getter films into the MEMS cavities to obtain and maintain the vacuum has been increasingly studied in the recent years.[6,7] Although some wafer-level packaging processes could allow multiple activation of the getter film, the getter film is usually thermally activated only once after cavity sealing with a background pressure typically in the 10^{-3}–10^{-1} mbar range. In this respect, it is quite different from the case of thermal activation of getter films used in ultrahigh vacuum chambers. During and after activation, the getter film must adsorb and trap undesired gases that were released during sealing-off the MEMS cavity (performed typically at 250–400 °C). During the device's lifetime, it must also pump residual gases to compensate surface outgassing, micro-leaks, and permeation which tend to increase the internal pressure of the cavity. For state of the art hermetic packaging processes, the amount of gas to be adsorbed mainly arises from packaging processing steps.

NEG materials such as titanium, vanadium, zirconium, and their alloys are usually deposited by sputtering. They are rapidly passivated by surface oxides in air and can be activated by annealing in vacuum[8,9] owing to bulk diffusion of their surface oxides. However, sputtered getter films incorporate rare gas atoms (usually argon),[10] and these atoms can be released during the cavity sealing process, limiting the vacuum level that can be reached. To avoid this issue, in this study, the getter films were deposited by e-beam evaporation. In order to increase the sorption capacity, getter films with a high porosity and surface roughness are desirable.[11–13] Li[11] deposited films on a tilted substrate and demonstrated that the larger the angle is the higher the porosity and the specific surface area of the getter film are. As a consequence, it was shown that a porous titanium film has a larger sorption capacity than a dense one. However, porous getter films still require an annealing either at a relatively high temperature or for a very long time because of their passivation by surface oxide. For example, Li[14] demonstrated that $Ti_{32}Zr_{15}V_{53}$ can be activated at 350 °C after 30 min, and Malyshev[15] reported that Ti-Zr-Hf-V can be activated at 150 °C after 24 h annealing, but such a long anneal time is not suitable for an industrial wafer-level packaging process. Alternatively, a thin protective layer such as Cu, Ag, Au, Ir, Os, Pd, or Pt can be used to cover the getter film to prevent its oxidation.[13] The activation of such composite getter films is obtained by out-diffusion of getter material atoms through the protective layer and their diffusion on the surface or/and by degradation of the protective layer, both of which lead to exposure of the underlying reactive material. In our previous works,[16–18] the interdiffusion phenomenon in the Au/Ti dense film has been studied and modelled. It was shown that an annealing temperature as low as 200 °C for 1 h can cause the out-diffusion of titanium atoms required to activate the getter film. However, the sorption capacity of the film is limited by the small specific surface area of such a dense getter film.

In this work, oblique deposition is employed to obtain porous titanium getter films which are then passivated *in situ*

a)mingwu.lille@gmail.com

with a thin gold overlayer deposited under normal incidence. The surface morphology, microstructure, and interdiffusion, between gold and porous titanium films, were investigated in detail by various techniques with the purpose of getting a larger sorption capacity at a low activation temperature.

II. EXPERIMENTAL DETAILS

Titanium and gold films were deposited by e-beam evaporation on Si (100) wafers. Prior to deposition, Si wafers were ultrasonically cleaned with acetone and ethyl alcohol and then dipped into piranha and buffered HF solutions to remove residues and native oxide, respectively. After cleaning, the substrates were immediately loaded into the evaporation chamber for deposition. A 100–200 nm thick titanium layer was first deposited with oblique angles of 0°, 30°, 50°, or 70°. Then, a 10–40 nm thick gold layer was deposited without breaking the vacuum under normal incidence. Deposition conditions are listed in Table I. After deposition, the films were annealed for 1 h at different temperatures in a rapid thermal annealing (RTA) chamber (Jipelec Jetfirst 100) at a vacuum level of 10^{-2} mbar. Such a vacuum level is similar to the one found in MEMS microcavities sealed at low temperatures. The annealing temperature was elevated at a rate of 80 °C/min, and the samples were kept at the target temperature for 1 h and then were cooled down under vacuum until the temperature reached 50 °C. In this work, the oxygen effective gettering ability of the layer is defined as the amount of oxygen atoms incorporated at the surface and inside the film resulting from residual oxygen and water vapor in the vacuum chamber during annealing and from the subsequent air exposure at room temperature and atmospheric pressure. This later contribution is considered to reflect the total remaining oxidizing gas sorption capacity of the film at room temperature after thermal activation. Because we performed thermal activation of the getter film in primary vacuum (as in the real case of vacuum packaging applications), this contribution is expected to be low with respect to oxidation occurring during thermal activation. This is quite different from the case of getter films activated in ultra-high vacuum where most of gas sorption occurs after activation. The total oxygen gettering ability was evaluated from oxygen content evaluation by Energy-Dispersive X-Ray (EDX) measurements. The precise background gas composition during annealing is not precisely known, but it is believed that the partial pressure of oxidizing species is sufficiently high, and it is not the limiting mechanism for surface oxidation. The surface morphology and cross section of the bilayer film were observed with a high-resolution Scanning Electron Microscope (SEM: Hitachi SU8000). The interdiffusion of the gold/titanium film was estimated from a resistance model of the bilayer film, where the total sheet resistance is measured with a four-point probe method. After being activated in a controlled environment similar to that of MEMS packaging, the oxygen effective gettering ability of the film was evaluated by Energy-Dispersive X-Ray Spectroscopy (EDX) in a Hitachi S-3600N SEM at 12 keV. The residual stress in the film was characterized by the wafer curvature method with a laser scanning system (FSM 500TC).

TABLE I. Deposition conditions of Au/Ti bilayers.

Material	Thickness (nm)	Angle deposition (deg)	Deposition rate (nm/s)	Pressure during deposition (Pa)
Titanium	200	70	1	7.3×10^{-6}
Gold	10	0	0.1	5.5×10^{-6}
Titanium	200	50	1	5.5×10^{-6}
Gold	10	0	0.1	6.1×10^{-6}
Titanium	200	30	1	5.6×10^{-6}
Gold	10	0	0.1	6.7×10^{-6}
Titanium	200	0	1	4.8×10^{-6}
Gold	10	0	0.1	5.6×10^{-6}
Titanium	100	50	1	6.7×10^{-6}
Gold	10	0	0.1	5.5×10^{-6}
Titanium	100	30	1	5.5×10^{-6}
Gold	10	0	0.1	5.7×10^{-6}
Titanium	100	0	1	6.0×10^{-6}
Gold	10	0	0.1	5.6×10^{-6}

III. RESULTS AND DISCUSSION

In oblique evaporation, a tilted columnar microstructure is formed due to the atomic shadowing effect. At the beginning of the deposition, discontinuous islands of the deposited material are first formed on the substrate, and then, nanocolumns are grown on these islands because the deposition atom flux arrives at the substrate surface at an oblique angle.[19] An additional variable is thus introduced into the growth process that has a significant influence on the development of the film's microstructure and compactness.

Because of ballistic deposition at a given oblique angle, a thin film with a microstructure of tilted and separated nanocolumns is formed. Experimentally, a tangent rule [Eq. (1)] (Ref. 20) is used to correlate the oblique angle of evaporation (α) and the tilt angle of the nanocolumns (β), both being defined from the substrate normal, as shown in Fig. 1(a)

$$\tan\alpha = 2 \times \tan\beta. \tag{1}$$

In an ideal case, the nanocolumns and voids are formed uniformly. Hence, the porosity of a film can be determined from the column separation in the film: it will be equal to the void width divided by the column spacing. If we consider that the column spacing is only due to the initial shadowing effect, from Fig. 1(b), it can be expressed by the following equation, where R is the radius of initial islands:

$$\text{porosity} = \frac{a}{b} = \frac{\frac{R}{\cos\alpha} - R}{\frac{R}{\cos\alpha} + R} = \frac{1 - \cos\alpha}{1 + \cos\alpha}. \tag{2}$$

The microstructure of films deposited with oblique angles (α) of 50° and 70° has been studied by SEM. SEM images of the samples surface and cross section are shown in Fig. 2. The inclination of the nanocolumns is clearly observed in SEM cross-sectional views. For the film deposited at 70° and 50°, measured angles (β) of 46° and 29° [Figs. 2(c) and 2(d)] are

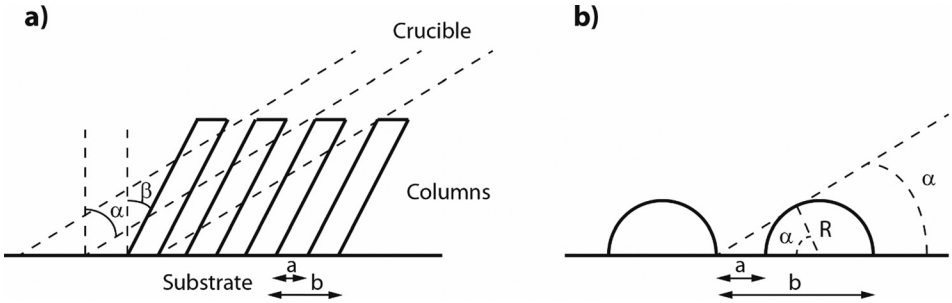

FIG. 1. (a) Definition of the incidence angle α of evaporation and of the tilt angle β of the nanocolumns. (b) Geometry of the initial shadowing for the estimation of column spacing.

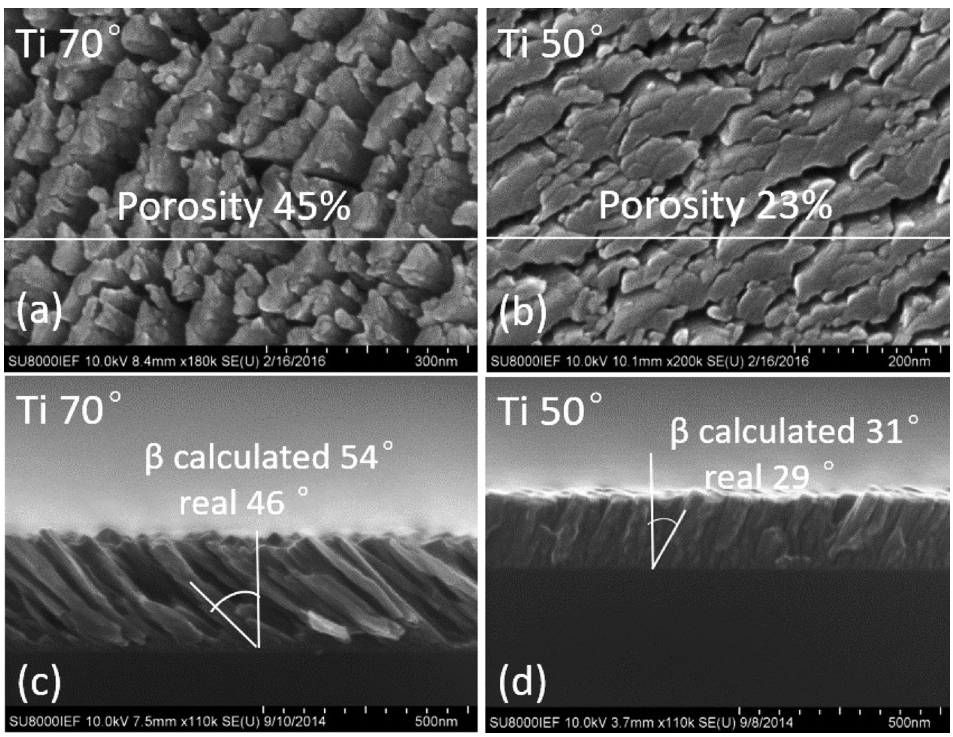

FIG. 2. SEM images of the surface and cross section of Ti with varying glancing angles 70° (a) and (c) and 50° (b) and (d) in the as-deposited state.

consistent with the calculated values of 54° and 31° using the tangent rule [Eq. (1)].

The porosity of the samples was estimated experimentally by two methods: (i) The weight of the sample was measured using a microbalance before and after removal of the film by HF etching, and the film thickness and area was evaluated from high resolution cross-section SEM images and top view optical images, respectively. Then, the density of the film was calculated from the weight to film volume ratio. (ii) For the same Ti film, the ratio of the void length to the column spacing measured on SEM images is the porosity. The results obtained by these two methods are gathered and compared in Fig. 3 with calculated values using Eq. (2). The plotted values are the relative porosity of the Ti films deposited at 50° and 70° with respect to the one of a dense film deposited at 0°. A good agreement is found between calculated and experimental values at 50° and, in a significantly lower extent, at 70° because the large film roughness at 70° limits the film thickness measurement accuracy. Both calculated and experimental results show, as expected, an increase in the Ti film porosity with the angle of incidence during evaporation.

A bare titanium film sample deposited with an oblique angle of 70° was characterized by EDX. The atomic oxygen content in the film after deposition and air exposure was found to be 55%. This is consistent with the measured column width (about 30 nm) and the expected native titanium oxide thickness along the surface of the column (about 5–10 nm according to Ref. 21). Thus, the high specific surface area of this film leads to its large oxidation after

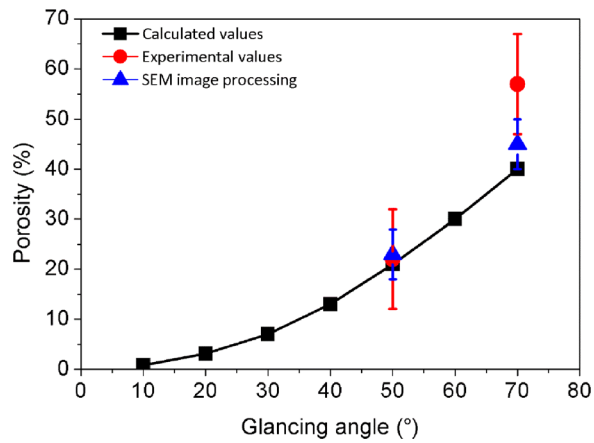

FIG. 3. Theoretical and experimental values of Ti film porosity as a function of the incidence angle of deposition (the error bars are the statistical deviation of measurements performed on 6 samples).

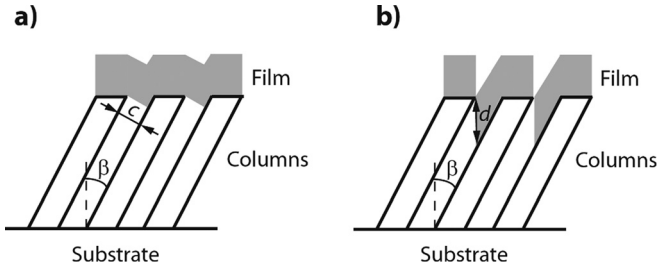

FIG. 4. (a) Schematic drawings showing the minimum film thickness required for the protection of a porous film with a tilted columnar structure. (a) Case of conformal deposition near the surface. (b) Case of purely directive deposition and normal incidence.

deposition and air exposure. This would limit the sorption capacity of the getter film after thermal activation by the bulk diffusion of surface oxide when integrated into the cavity of a MEMS wafer-level packaging. To avoid such an oxidation, a thin gold layer deposited *in situ* was investigated as a protective layer against oxidation. For such a bilayer getter, thermal activation is achieved by Ti out-diffusion through the gold film as demonstrated in previous works.[16–18]

Ideally, the gold film must be as thin as possible but must completely cover the surface of the porous getter film. For a conformal deposition near the surface, the minimum Au film thickness would be the normal distance c between two tilted columns [Fig. 4(a)], which can be calculated from the measured width of the columns and from α (or β). Likewise, for a purely directive deposition at normal incidence, the minimum Au film thickness would be the vertical gap d between two columns [Fig. 4(b)]. In the real case of a partially conformal deposition at normal incidence, the minimum gold thickness required is between these 2 limits. The calculation shows that the minimum gold thickness required for a Ti film deposited at 50° would be in the 8–12 nm range at 50° and in the 20–30 nm range for a film deposited at 70°. The EDX measurement listed in Table II shows that 10 nm of gold efficiently prevents oxidation of titanium samples deposited at 0°, 30°, and 50° as no oxygen peak was detected. As illustrated in Fig. 5 for the Ti film deposited at 50°, this was confirmed by XPS analysis, showing none oxygen nor titanium in the analysis depth (~5 nm).

TABLE II. EDX analysis of as-deposited $Au_{10\,nm}/Ti_{200\,nm}$ films. (Ti deposited at 0°, 30°, 50°, and 70° angles of incidence and Au deposited under normal incidence).

	Ti (%)	Au (%)	O (%)
Ti with 0° tilt	94	6	Below detection limit
Ti with 30° tilt	94	6	(confirmed by XPS)
Ti with 50° tilt	94	6	
Ti with 70° tilt	48	4	48

Instead, for the sample deposited at 70°, 48% of oxygen is found even with an increased thickness of 40 nm of the gold layer, indicating a large oxidation of the titanium after air exposure. This suggests that the film deposited at a high oblique angle becomes too porous for an efficient passivation of its surface by a thin gold film. A thicker gold film could be used, but this would lead to a large increase in the temperature required for thermal activation. Since a thin gold film can prevent oxidation of the porous titanium film only for oblique angles smaller or equal than 50°, $Au_{10\,nm}/Ti_{100\,nm}$ and $Au_{10\,nm}/Ti_{200\,nm}$ bilayers with titanium deposited at 0°, 30°, and 50° were further studied and compared.

First, the effective oxygen gettering ability of these films, defined in this work as the total amount of incorporated oxygen in the surface and inside the film, was evaluated by EDX.

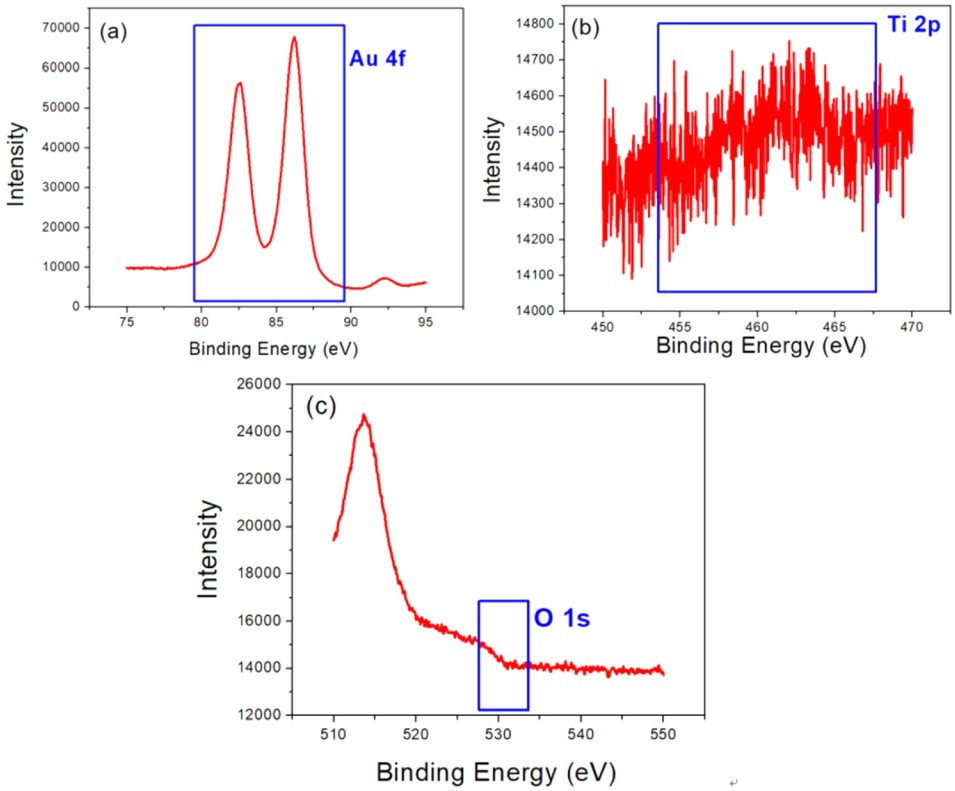

FIG. 5. XPS analysis of the Au(10 nm)/Ti sample with the Ti layer evaporated at an angle of incidence of 50°. (a) Au4f peak, (b) Ti2p peak, and (c) O1s peak.

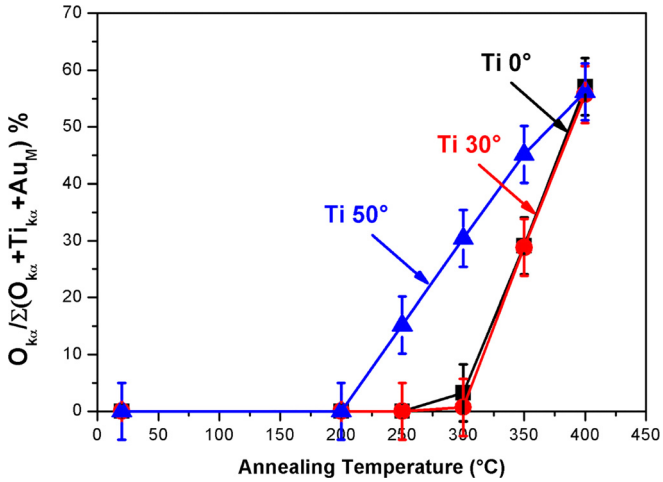

FIG. 6. Normalized variations of O in $Au_{10\,nm}/Ti_{200\,nm}$ bilayers as a function of 1 h annealing temperature under vacuum for evaporation angles equal to 0°, 30°, and 50°. The error bars represent the measurement error.

The oxygen content in the films is plotted in Fig. 6 as a function of annealing temperature for various angles of incidence during deposition. As mentioned above, before annealing, there is no contamination in the film, even for an oblique deposition angle of 50°. After vacuum annealing at 300 °C for 1 h followed by air exposure, the EDX measurement shows that the oxygen content increases up to 30% for the sample deposited with an angle of 50°, but for other films, it remains lower than 8%. This demonstrates that Au/Ti bilayer getter films deposited at an oblique angle at 50° can significantly increase the oxygen effective gettering ability. As detailed below, it is considered that Au/Ti interdiffusion is promoted by the porous Ti structure during the low temperature anneal, which exposes the underlying titanium and enhances gas absorption. Indeed, as shown in Fig. 7, an interdiffusion of gold and titanium is observed in SEM surface and cross-sectional views using backscattered electron (BSE) detection. After annealing at 300 °C for 1 h, the film surface is no longer uniform (Fig. 7 top), indicating a non-homogeneous interdiffusion. As evidenced by the dark and bright features in BSE images, for both Au/Ti films deposited at 0° and 50°, gold forms islands at the surface and titanium oxide exhibits flakes. As detailed previously in the case of Ti films evaporated under normal incidence,[17] during annealing, Ti atoms mainly diffuse through the gold film grain boundaries and are then oxidized when they reach the surface. Oxidation of out-diffused Ti atoms which can occur at 10^{-2} mbar provides an additional driving force for further Ti diffusion though Au because of the asymmetric concentrations of Ti below and above the gold film. Because of the very low diffusion length of oxygen in Ti at room temperature, the subsequent oxidation during air exposure at room temperature and atmospheric pressure is expected to be very limited and much lower than during annealing. This is expected for most gases except for hydrogen because its sorption is reversible. From EDX results shown in Fig. 6, it is found that if the titanium is dense (deposition at 0°), only a little titanium oxide is formed at the surface after annealing at 300 °C for 1 h. Instead, for the porous titanium deposited with an angle of 50°, the oxygen content increases to about 30%. This indicates a bulk oxidation of porous titanium arising from a highly discontinuous gold film at the surface after annealing and the large specific area of the Ti porous film. For titanium deposited at 0°and annealed at 400 °C for 1 h, the gold layer is buried under a quasi-continuous 40 nm thick titanium oxide layer. However, as seen in Fig. 7 (right), the diffusion and oxidation are more significant in the porous titanium film deposited at 50°, leading to a thicker layer of titanium oxide (60 nm) at the surface. This TiO_2 thickness is also larger than the one measured on a dense Ti film with a 5 nm Au layer.[16] This shows that Ti porosity increases the effective gettering ability of the titanium getter. It is attributed to a larger interdiffusion of titanium and gold and a larger oxidation. We think that it is not due to a thinner Au layer nor to a higher diffusion coefficient of Ti in Au but due to the larger Ti surface in contact with Au

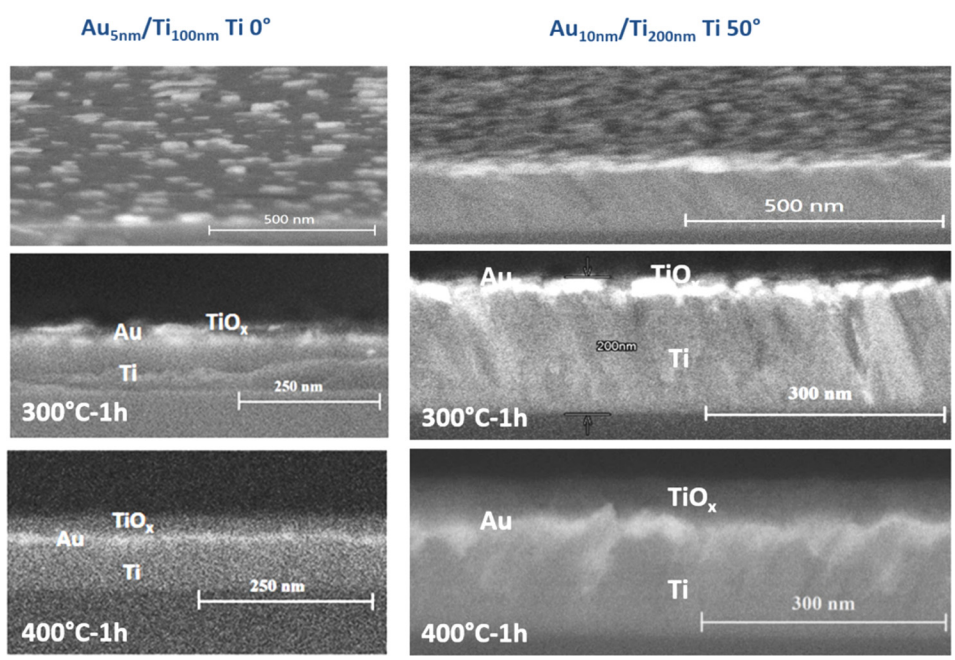

FIG. 7. SEM images (BSE mode) of the surface (top) and cross section of the Au/Ti sample after annealing at 300 °C (middle) and 400 °C (bottom) at normal incidence (left) and with an incidence angle of 50° (right).

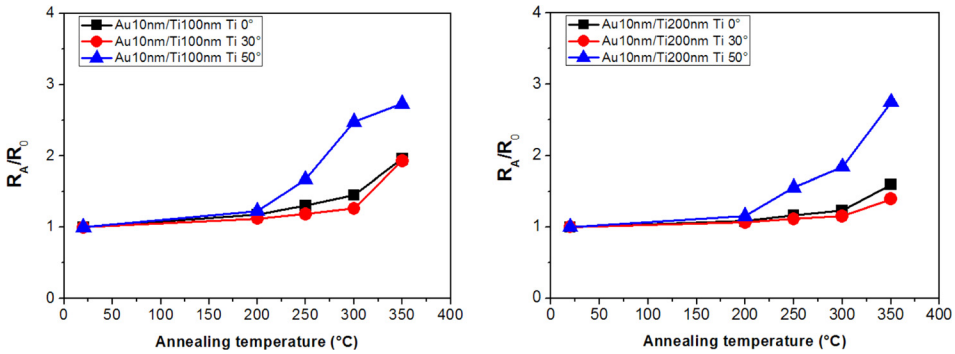

FIG. 8. Normalized sheet resistance versus annealing temperature for different evaporation angles of incidence of (a) $Au_{10\,nm}/Ti_{100\,nm}$ and (b) $Au_{10\,nm}/Ti_{200\,nm}$ samples.

(see Fig. 4), a larger thermal degradation of the Au film (loss of continuity), and to the larger specific area of the porous Ti film exposed to gas.

Finally, the sheet resistance of Au/Ti samples was measured to evaluate the interdiffusion and effective gettering ability of Au/Ti films after annealing at various temperatures. The evolution of the normalized sheet resistance (R_A/R_0) as a function of the annealing temperature is plotted in Fig. 8 for $Au_{10\,nm}/Ti_{100\,nm}$ and $Au_{10\,nm}/Ti_{200\,nm}$ samples, where R_0 and R_A are the sheet resistances of as-deposited samples and of annealed samples, respectively.

The results show that the normalized sheet resistance increases monotonically with annealing temperature for both titanium thicknesses. It increases slowly up to about 300 °C for 0° and 30° deposition angles, while the increase is more significant as of 250 °C for the 50° deposition angle. These sheet resistance variations are assumed to result from a thickness decrease of the underlying conductive titanium layer due to out-diffusion of titanium through the gold passivation layer and their subsequent oxidation when they are exposed to traces of oxidizing species during annealing and when they are exposed to ambient air.[16]

An estimation of how deep oxidation proceeds in the Ti porous layer was performed by comparing the results obtained for the Au (10 nm)/Ti samples with 100 nm and 200 nm thick Ti films with the help of the model shown in Fig. 9.

The total resistance of the initial thicker bilayer $Au_{10\,nm}/Ti_{200\,nm}$ can be considered as parallel resistances of an upper part $Au_{10\,nm}/Ti_{100\,nm}$ and a lower part $Ti_{100\,nm}$, as shown in Fig. 9 (left). After annealing, titanium atoms diffused through the gold layer and formed titanium oxide at the surface with possibly a partial deep oxidation of the Ti film remaining below. Thus, after annealing, the resistance of an $Au_{10\,nm}/Ti_{200\,nm}$ sample can be considered as constituting two parts (Fig. 9): the upper part R1 is like the resistance R3 of an $Au_{10\,nm}/Ti_{100\,nm}$ sample after annealing (Fig. 9 Bottom) and the bottom part is an underlying titanium layer (R2 in Fig. 9). If we assume that interdiffusion and oxidation phenomena are similar for the thicker and thinner samples, then $R_1 = R_3$. The resistance R2 of the 100 nm thick underlying titanium can thus be expressed as indicated in the following equation:

$$\frac{1}{R_{Ti\,100\,nm}} = \frac{1}{R_2} = \frac{1}{R_{200}} - \frac{1}{R_{100}}. \tag{3}$$

The extracted normalized resistivity of the underlying 100 nm thick bottom titanium layer versus annealing temperature for samples with 10 nm of gold covering titanium deposited at 0° and 50° is given in Fig. 10. For samples without oblique deposition and annealed below 400 °C, the extracted resistivity of this underlying titanium layer is, as expected, nearly constant. On the contrary, for titanium deposited at 50°, the resistivity of this bottom part of the underlying titanium layer increases monotonically with annealing temperature. This shows that the underlying 100 nm thick bottom part of the 200 nm thick Ti layer of the 200 nm samples is partly oxidized after annealing above 300 °C. A deep diffusion of oxidizing gases thus occurs in annealed porous Ti samples. This is clearly favorable to get a good gas sorption capacity.

The getter film is intended to be integrated in the cavity of a wafer level package. Its mechanical stress must then be considered as it might affect its adhesion and lead to cap deformation. This later effect could be detrimental for the

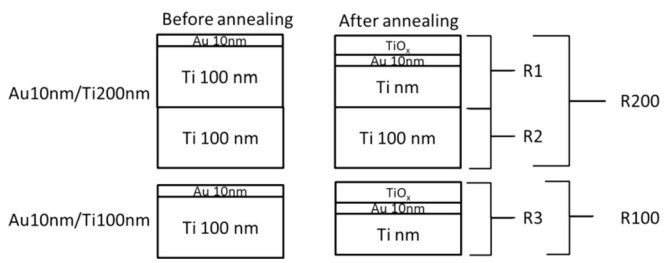

FIG. 9. Model of the parallel electrical resistances before and after annealing for $Au_{10\,nm}/Ti_{200\,nm}$ and $Au_{10\,nm}/Ti_{100\,nm}$ bilayers.

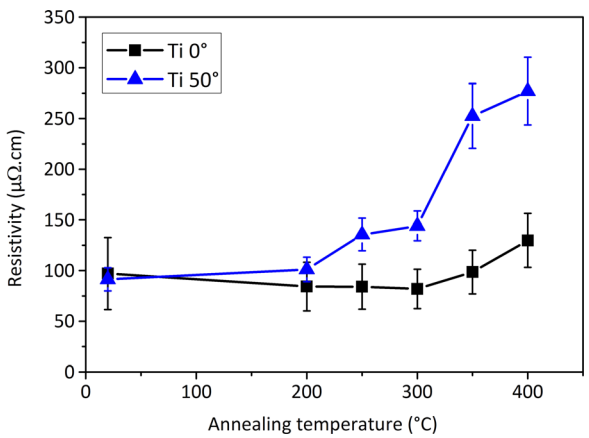

FIG. 10. Normalized resistivity of the underlying bottom titanium layer versus annealing temperature for different incidence angles.

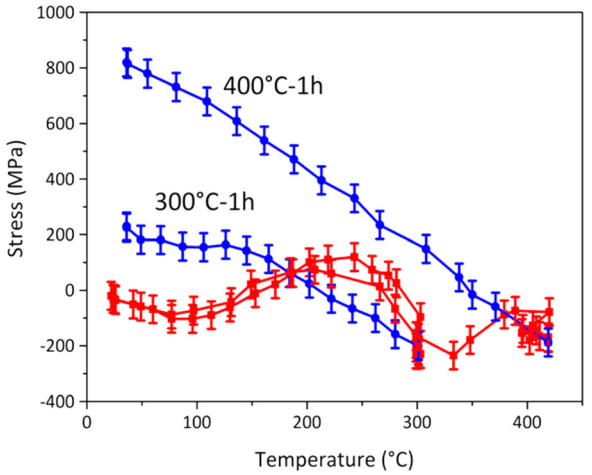

FIG. 11. Stress in $Au_{10\,nm}/Ti_{200\,nm}$ (Ti deposited at 50°) versus temperature during heating (red) and cooling (blue) after a stage of 1 h at 300 °C or 400 °C.

sealing rings and the encapsulated devices. The film stress was evaluated by using the substrate curvature method based on the Stoney formula.[22] The stress variations in $Au_{10\,nm}/Ti_{200\,nm}$ (Ti 50°) films, measured at atmospheric pressure under N_2 flow during temperature cycles up to 300 °C and 400 °C, are plotted in Fig. 11. The heating rate was 10 °C/min, the temperature was maintained constant for 1 h at 300 °C or 400 °C, and then, the cooling was free until room temperature. The residual stress in as-deposited bilayers is very low. During the heating step, film stress has a complex variation going from more compressive, more tensile, and then more compressive stress than in as-deposited films. During cooling, the stress variation is roughly linear towards a more tensile stress in agreement with a stress variation dominated by thermomechanical stress. This is expected as the linear thermal expansion coefficients of Ti, Au, and TiO_2 are all larger than the silicon wafer one. After cooling down to ambient temperature, the getter film residual stress is tensile. For the sample activated at 400 °C, the tensile stress reaches 800 MPa, while it is around 200 MPa for the sample activated at 300 °C. This clearly shows that the activation temperature of the proposed Au/porous Ti getter film must be minimized for its integration in the cavity of a wafer level package.

IV. CONCLUSION

In this work, we investigated Au/Ti bilayers with a porous Ti film deposited by evaporation with different oblique angles for their use as getter films for vacuum wafer-level packaging. The Ti films have a tilted columnar structure with a porosity up to 50%. It is demonstrated that a 10 nm thick Au film deposited under normal incidence is able to fully cover the Ti porous films and to protect them against oxidation provided that the Ti deposition angle is lower or equal to 50°. During thermal treatment, an inhomogeneous interdiffusion of gold and titanium, promoted by porosity, breaks this protection layer and exposes porous titanium which acts as an efficient getter. As demonstrated by the measurement of incorporated oxygen at the surface and in the bulk, Au/Ti bilayers with Ti films deposited at 50° are promising low temperature getter films as they have a large effective gettering ability after a thermal activation at 300 °C for 1 h and a not excessive residual stress (200 MPa) after thermal activation.

ACKNOWLEDGMENTS

This work was partly supported by the French National Research Agency (ANR) in the frame of the "PRESTIGE" project (No. ANR 12 RMNP 0010), the Natural Science Foundation of Jiangsu Province of China (No. BK20170340), and the Natural Science Fund for Colleges and Universities in Jiangsu Province of China (No. 17KJB510049). Most of the experiments were performed in C2N clean room facilities supported by the Renatech network, and the authors wish to thank the C2N process engineers and technicians for their assistance. The authors wish to thank Professors Mingxiang Wang and Dongli Zhang from Soochow University for valuable discussions.

[1]M. Elßner, "Vacuum quality evaluation for uncooled micro bolometer thermal imager sensors," Microelectron. Reliab. **54**, 1758 (2014).
[2]G.-D. Anna, "Miniature and MEMS-type vacuum sensors and pumps," Vacuum **83**, 1419 (2009).
[3]B. Zhang, Y. Wang, W. Wei, L. Fan, J. P. Wang, and W. M. Li, "Deposition and characterization of Ti-Zr-V non-evaporation getter films," Phys. Procedia **32**, 802 (2012).
[4]Y. C. Kim, D.-K. Paik, N.-S. Kang, K.-Y. Kim, and M.-H. Park, "Gettering of gas molecules in the frit sealed glass panel by thin film metal coatings," in *Proceedings of the IEEE Vacuum Microelectronics Conference* (2001), p. 205.
[5]E. Giorgi, B. Ferrario, and C. Boffito, "High-porosity coated getter," J. Vac. Sci. Technol., A **7**, 218 (1989).
[6]L. Tenchine, X. Baillin, C. Faure, P. Nicolas, E. Martine, and A.-M. Papon, "NEG thin films for under controlled atmosphere MEMS packaging," Sens. Actuators, A **172**, 233 (2011).
[7]C. Vivek, L. Xie, and B.-T. Chen, "Titanium-based getter solution for wafer-level MEMS vacuum packaging," J. Electron. Mater. **42**(3), 485 (2013).
[8]C. Benvenuti, P. Chiggiato, P. C. Pinto, A. E. Santana, T. Hedley, A. Mongelluzzo, V. Ruzinov, and I. Wevers, "Vacuum properties of TiZrV non-evaporable getter films," Vacuum **60**, 57 (2001).
[9]C. Benvenuti, P. Chiggiato, F. Cicoira, and Y. L'Aminot, "Nonevaporable getter films for ultrahigh vacuum applications," J. Vac. Sci. Technol. **16**, 148 (1998).
[10]X. Liu, M. Adam, Y. He, and Y. Li, "Vacuum pumping performance comparison of non-evaporable getter films deposited using argon and krypton as sputtering gases," in *Proceedings of the IEEE Particle Accelerator Conference, Knoxville, USA* (2005), p. 2860.
[11]C.-C. Li, J.-L. Huang, R.-J. Lin, H.-K. Chang, and J.-M. Ting, "Fabrication and characterization of non-evaporable porous getter film," Surf. Coat. Technol. **200**, 1351 (2005).
[12]Y. Xu, J. Cui, H. Cui, H. Zhou, Z. Yang, and J. Du, "ZrCoCe getter films for MEMS vacuum packaging," J. Electron. Mater. **45**(1), 386 (2016).
[13]J. C. Souriau, E. Dlevoye, F. Baleras, and D. Henry, "Thin film getter protection," U.S. patent 0,213,539 (4 September 2008).
[14]C. C. Li, J. L. Huang, R. J. Lin, and D. F. Lii, "Preparation and characterization of non-evaporable porous Ti-Zr-V getter films," Surf. Coat. Technol. **201**, 3977 (2006).
[15]O. B. Malyshev, R. Valizadeh, R. M. A. Jones, and A. Hannah, "Effect of coating morphology on the electron stimulated desorption from Ti-Zr-Hf-V nonevaporable-getter-coated stainless steel," Vacuum **86**, 2035 (2012).
[16]M. Wu, J. Moulin, S. Lani, G. Hallais, C. Renard, and A. Bosseboeuf, "Low temperature activation of Au/Ti getter film for application to wafer-level vacuum packaging," Jpn. J. Appl. Phys., Part 1 **54**, 030220 (2015).
[17]M. Wu, J. Moulin, G. Agnus, and A. Bosseboeuf, "Low activation temperature Au/Ti getter films for wafer-level vacuum packaging," ECS Trans. **64**(5), 297 (2014).

[18]M. Wu, J. Moulin, P. Coste, S. Perrot, J.-L. Perrossier, C. Renard, and A. Bosseboeuf, "Comparative study of Au/Ti, Au/V and Au/Zr films oxygen gettering ability," Thin Solid Films **616**, 543 (2016).
[19]A. G. Dirks and H. J. Leany, "Columnar microstructure in vapor-deposited thin films," Thin Solid Films **47**, 219 (1977).
[20]J. M. Nieuwenhuizen and H. B. Haanstra, "Microfractography of thin films," Philips Tech. Rev. **27**, 87 (1966).
[21]E. Gemelli and N. H. A. Camargo, "Oxidation kinetics of commercially pure titanium," Rev. Mater. **12**(3), 525 (2007).
[22]G. C. A. M. Janssen, M. M. Abdalla, F. van Keulen, B. R. Pujada, and B. van Venrooy, "Celebrating 200th anniversary of the Stoney equation for film stress: Developments from polycrystalline steel strips to single crystal silicon wafers," Thin Solid Films **517**(6), 1858 (2009).